Korean J. Chem. Eng., **30**(4), 878-890 (2013)
DOI: 10.1007/s11814-012-0185-y

Thermal degradation characteristic of Tetra Pak panel boards under inert atmosphere

Aysel Kantürk Figen*, Evren Terzi, Nural Yilgör***, Saip Nami Kartal**, and Sabriye Pişkin*,†**

*Department of Chemical Engineering, Yildiz Technical University, 34210 Davutpasa, Istanbul, TURKEY
**Department of Forest Biology and Wood Protection Technology, Forestry Faculty, Istanbul University, 34473 Bahcekoy, Istanbul, TURKEY
***Department of Forest Products Chemistry and Technology, Forestry Faculty, Istanbul University, 34473 Bahcekoy, Istanbul, TURKEY
(*Received 4 June 2012 • accepted 3 November 2012*)

Abstract−Thermal degradation characteristics of Tetra Pak panel boards (TPPB) can be useful to improve usage of such panels as an alternative to wood-based products such as plywood, fiberboard, and particleboard. In the study, samples from the TPBBs manufactured from waste Tetra Pak packages (WTPP) were heated in a nitrogen atmosphere at different heating rates (10, 15 and 20 °C/min) using a thermal analysis system. The Coats-Redfern kinetic model was applied to calculate kinetic parameters. The degradation rate equations were then established. In addition, the kinetic compensation effect (KCE) was used to correlate the pre-exponential factor (k_o) with activation energy (E_a) and the existence of the KCE was accepted. TG-FT/IR analyses were applied to the TPPB degradation and then the FT-IR stack plot was used to analyze gas products (CO_2, CH_4, HCOOH, and CH_3OH). Infrared vibrational frequencies and the micro, crystal structure of the TPPBs were investigated by Fourier transform infrared spectroscopy (FT-IR), Scanning electron microscope (SEM) and X-Ray diffraction analysis (XRD), respectively.

Key words: Tetra Pak, Panel Board, Thermal Degradation, Coats-Redfern, FT-IR

INTRODUCTION

Tetra Pak packaging is a beverage and liquid food system widely used all over the world as an aseptic packaging material. Tetra Pak is currently used for delivery and safe packaging of food products without any need for refrigeration or preservation. In 2007, more than 137 billion Tetra Pak packages were produced and sent worldwide, while in 2008 this number increased to 141 billion. In light of these numbers, recycling of Tetra Pak packaging becomes an important concern in the control of municipal solid wastes (MSW) [1-6].

Nowadays, waste Tetra Pak (WTP) is recycled by different methods [1,7-10]:

(1) Recovery of waste cellulose (paper): Tetra Pak is recycled through a simple, well-established process called hydro-pulping where thin layers of plastic (low density polyethylene-LDPE) and aluminum are separated from paper parts (cellulose fibers and high quality fibers) are then used in the production of paper products.

(2) Recovery of Aluminum (Al): Aluminum in the waste is recovered by applying pyrolysis processes in ovens. The plasma plant is fed with polyethylene (PE)/Al residues, from which the cellulose fibers have been previously removed, and PE is transformed into paraffin and the aluminum is recovered in its pure form. The plasma process is clean, and there is no need for the addition of any compound, such as salt. In principle, a higher recovery rate of aluminum is attainable, since no oxidation of the aluminum occurs during the process.

(3) Recovery of LDPE: The polyethylene/aluminum fraction is first washed and then sent to a plastic regeneration plant to produce a new semi-finished product called ecoAllene, a sturdy, versatile plastic that is packaged and sold in granular form.

In addition to these options, WTPP can be used to produce TTPB, which can be used as construction materials such as separation panels, roof construction panels, construction molds and transportation containers. Considering the above-mentioned recycling methods, the production of panel boards from WTPP is a cost-effective application for recycling such waste without advance processing such as hydro-pulping or plasma technology. WTPP can be converted to such commercial products by performing shredding, scraping and molding treatments which are not costly compared with other recycling options. Such panel products produced from WTPP may help reduce usage of wooden raw materials to produce wood based panels, thus decreasing the pressure on forests.

To increase the usage and quality of TPPBs, it is necessary to investigate their thermal properties, which are very important in determining their possible future usage areas. TPPB is a thermally degradable and combustible material due to its chemical substance. Thermal degradation characteristic affects the degradation and performance of TPPB products. Thermal characteristic should be considered in determining usage area. However, for TPPB requiring stability, the thermal degradation temperature is an upper limit for practical use. It is not possible to use the TPPB at temperature below which thermal decomposition occurs. Also, many materials produce gases on thermal degradation, and gases strongly affect the degradation kinetics. Therefore, knowledge of the thermal degradation of TPPB can be critical in many practical applications.

Although pyrolysis of waste Tetra Pak has been studied extensively, there is a lack of study on the thermal degradation behavior of TPPBs.

In a previous study, pyrolysis experiments were carried out in an

†To whom correspondence should be addressed.
E-mail: piskin@yildiz.edu.tr, sabriyepiskin@gmail.com

Fig. 1. Image of tetra pak panel board.

Table 2. Proximate analyses of the tetra pak panel board

Moisture/ %	Ash/ %	Volatile mater/%	Fixed carbon/%	Calorific values/MJkg^{-1} (on the dry basis)
2.90	6.19	86.00	4.91	30.30

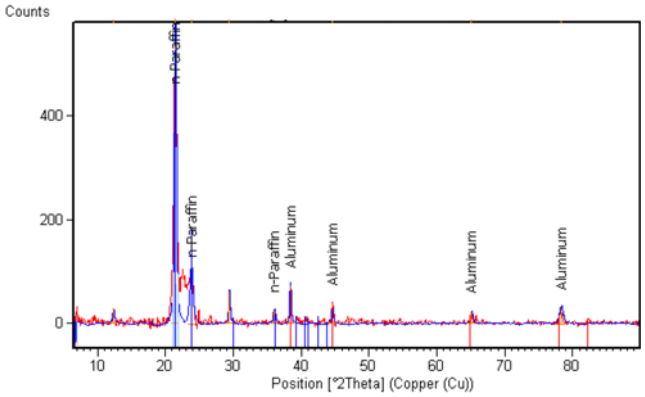

Fig. 2. XRD pattern of tetra pak panel board.

inert atmosphere in a batch reactor at different temperatures and by different pyrolysis modes (one- and two-step). The char obtained from pyrolysis was suitable to use as solid fuel because of its high calorific value and low ash content. Different types of gas were produced mostly from the degradation of cardboard and contained a high proportion of carbon oxides. TGA results showed that pyrolysis of Tetra Pak consisted of two distinct stages [1]. The pyrolysis of Tetra Pak in nitrogen atmosphere was investigated with a thermogravimetric analysis (TGA) reaction system. The pyrolysis kinetic experiments for the Tetra Pak and its main components (Kraft paper and LDPE) were carried out at heating rates (β) of 5.2, 12.8, 21.8 K min^{-1}. The results indicated that the one-reaction model and two-reaction model could be used to describe the pyrolysis of LDPE and Kraft paper respectively. The reaction was contributed to mainly by the pyrolysis reaction of LDPE. In the XRD analysis, the results indicated that pure aluminum foil could be obtained from the final residues [4].

In addition, the pyrolysis reactions of Tetra Pak were performed in four different oxygen concentrations (O_2) of 5.4, 10.4, 14.8, and 21.0%. This was done to better analyze the pyrolysis and gaseous products collected at room temperature (298 K) and analyzed by gas chromatography (GC). It is suggested that since the synthetic gases (CO, CO_2, H_2O, HCs) contained a high calorific value, their usage as marketable fuels greatly supported the importance of energy recovery from post-consumer Tetra Pak packages [2].

In the present study, thermal stability of TTPBs produced from waste Tetra Pak was investigated under a nitrogen atmosphere. Coats-Redfern, non-isothermal kinetic model, was applied to the calculations to establish kinetic parameters used in the rate equations. In addition, evolved gas analysis was examined to characterize the main compounds released during the thermal degradation by the TG-FT/IR analysis.

EXPERIMENTAL

1. Material and Characterization

TPPBs were supplied from YEKASAN Converting Factory in Izmir, Turkey (Fig. 1). For panel production, waste Tetra Pak was shredded and pressed in a hot press at 180 °C and a pressure of 1.2 N/mm^2 for 12 min to 18 mm of target panel thickness. Physical and

Table 1. Physical and mechanical properties of the tetra pak panel board

Properties	Value	Standards
Specific gravity, g/cm^3	1.09	TS 180
Swelling in thickness (2 hour at 20 °C water), %	1.04	TS180
Swelling in thickness (24 hour at 20 °C water), %	5.04	TS180
Bending Strength, kPa/cm^2	186.5	TS180
Tensile strength perpendicular to the surface, kPa/cm^2	3.50	TS180
Tensile strength parallel to the surface, kPa/cm^2	72.8	ASTM 1037
Screw holding strength (perpendicular to the surface), kPa	87.5	TS10505
Janka hardness, kPa/cm^2	681.5	BS 1811
Density, g/cm^3	1.10	DIN 52361
Heat insulation coefficient, W/mK	0.13	DIN 52612
Longitudinal bending, N/mm^2	19.00	DIN 68761
Transverse deflection, N/mm^2	2.25	DIN 68761

mechanical properties of TPPBs are listed in Table 1. TPPBs contain 74±1% of Kraft paper, LDPE of 22.5±1.87% and aluminum of 6±1%. The approximate analyses of the samples were performed in accordance with the ASTM standard (ASTM E1131-03), and the calorific value was determined in accordance with ASTM D 5865-04 by a bomb calorimeter (IKA-Calorimeter C400) (Table 2). The average of three samples was used for all below-mentioned analyses.

Also, in order to investigate the effect on fabrication process on degradation behavior of TPPBs, thermal analyses were performed on WTPP under the same conditions.

Crystal structure, infrared vibrational frequencies and microstructure of stalks were investigated by X-Ray diffraction analysis (XRD), Fourier transform infrared spectroscopy (FT-IR), and scanning electron microscope (SEM), respectively. Characterization techniques for structural analyses in the present study are listed below:

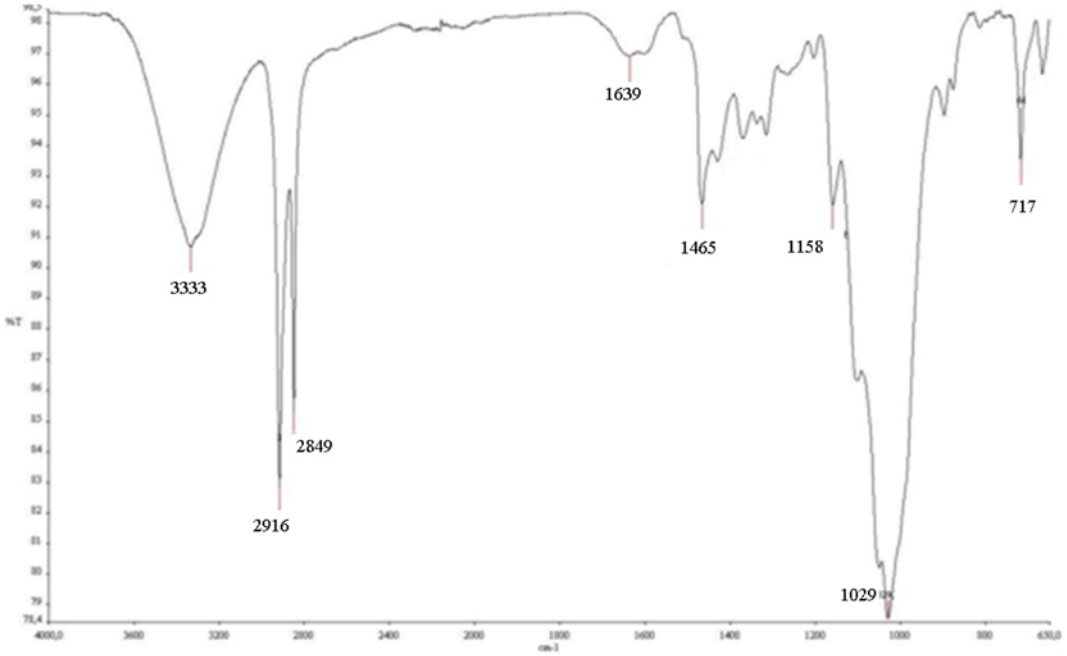

Fig. 3. FT-IR spectrum of tetra pak panel board.

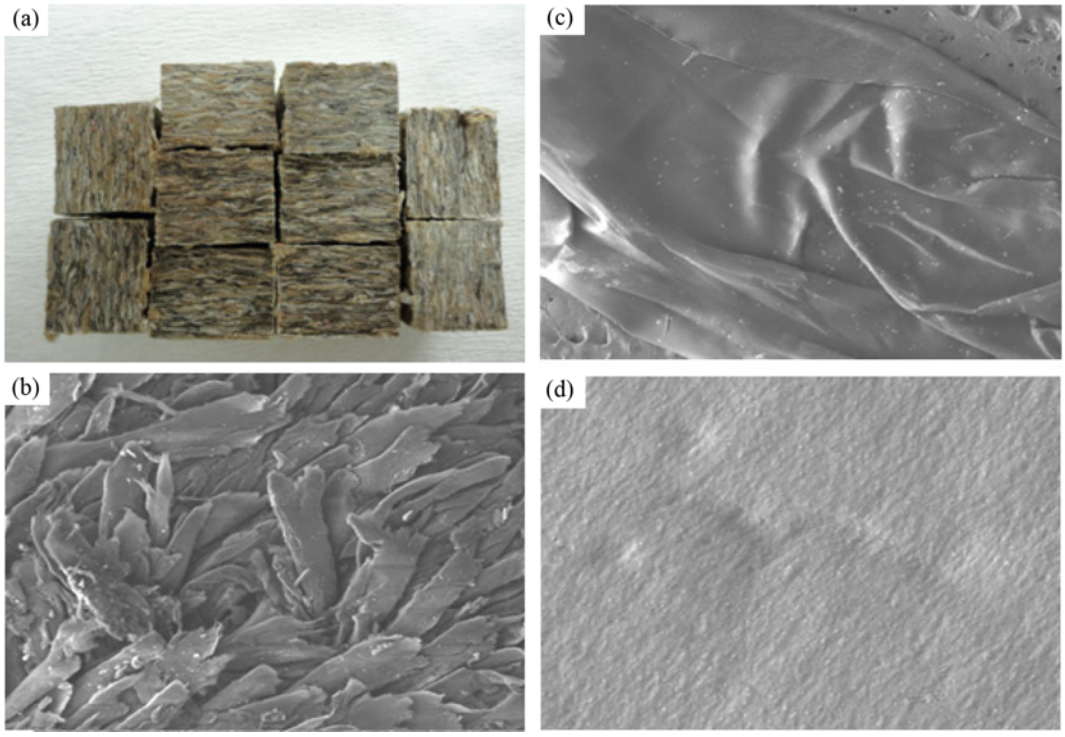

Fig. 4. SEM images of tetra pak panel board.

1-1. XRD Analysis

Crystal structure of sample was determined by the XRD technique. XRD analysis was carried out at an ambient temperature using a Philips Panalytical X'Pert-Pro diffractometer in a range of diffraction angles from 5° to 40° with CuKα radiation at operating parameters of 40 mA and 45 kV. The XRD pattern is given in Fig. 2.

1-2. FT-IR Analysis

Attenuated total reflectance (ATR) of FT-IR spectroscopy (Perkin Elmer Spectrum One) was used to determine the infrared vibrational frequencies. Before analysis, the crystal area was cleaned and the background reading collected. The material was then placed over the small crystal area on a universal diamond ATR top-plate. Force was then applied to the sample, pushing it onto the diamond surface. The resulting FT-IR spectrum was recorded in the spectral range of 4,000 to 650 cm^{-1} at ambient temperature; the resolution used was 4 cm^{-1}. The FT-IR spectrum is given in Fig. 3.

1-3. SEM Analysis

The microstructure of the material was investigated by SEM

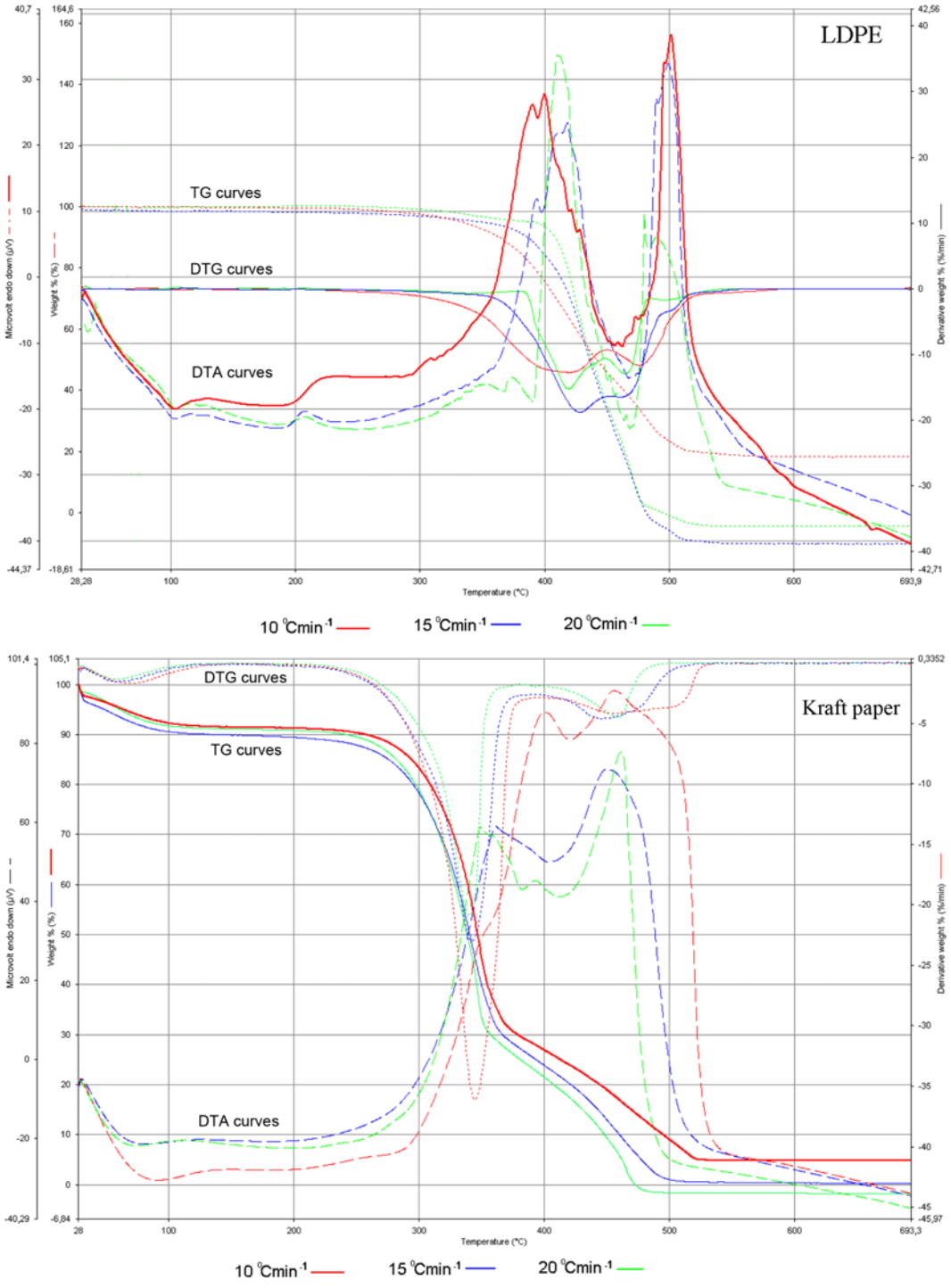

Fig. 5. Thermal analysis curves of tetra pak panel board components at different heating rates.

(Chemscan/Apollo300) analysis. The sample was made ready for analysis by fixing it to the device's sample holder with the help of a carbon sticky band and then coating it with a small amount of conductive material (Au). The SEM images are given in Fig. 4.

2. Thermal Degradation Characteristic

Thermal degradation characteristics of the WTPP and its components, TPPBs and its components were carried out using the Perkin Elmer Diamond thermal analysis instrument, which was calibrated using the melting points of indium (T_m=156.6 °C) and tin (T_m=231.9 °C) under the same conditions as the sample. The analyses were done at different heating rates of 10, 15 and 20 °C/min in an atmosphere of N_2 that had a constant flow rate of 100 ml/min. The samples (~5 mg) were allowed to settle in standard alumina crucibles and heated to 700 °C. In the first step of the thermal analysis, the TPPBs were separated into layers and LDPE, Kraft paper and aluminum foil were obtained. Thermal degradation characteristics of LDPE and Kraft paper were carried out under the same conditions to determine their thermal degradation behavior. Thermal analysis curves of TPPBs at different heating rates are given in Fig. 5. In addition, the TG and DTG curves of the TPPBs, Kraft paper and LDPE were compared at a 15 °C/min^{-1} heating rate. The results are given in Fig. 6.

In the second step of the thermal analysis, cryogenic grinding was applied to the WTPP and TPPBs in order to obtain a homogeneous specimen for thermal analysis. TG and DTG profiles of are

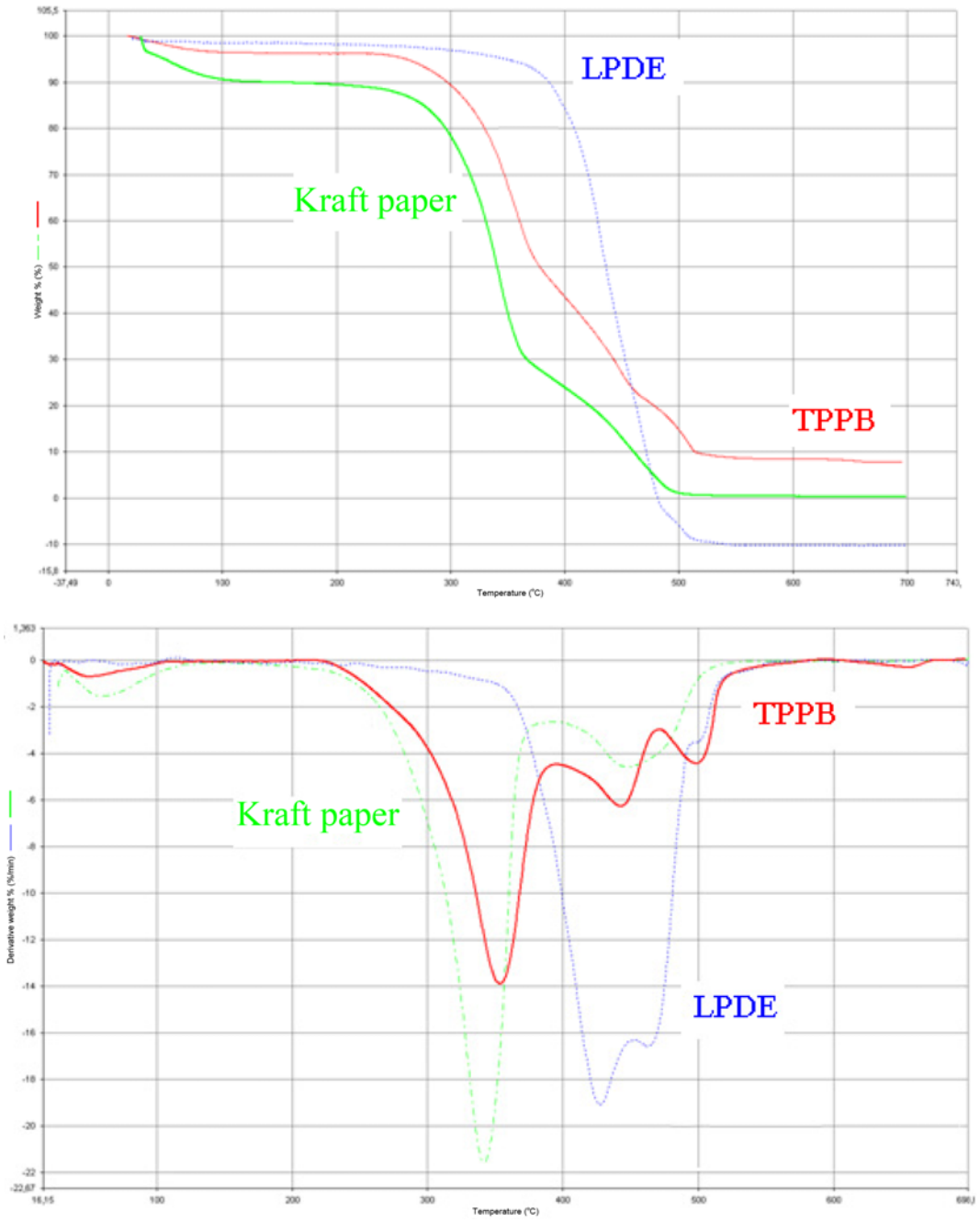

Fig. 6. Compared TG and TDG curves at 15 °C/min.

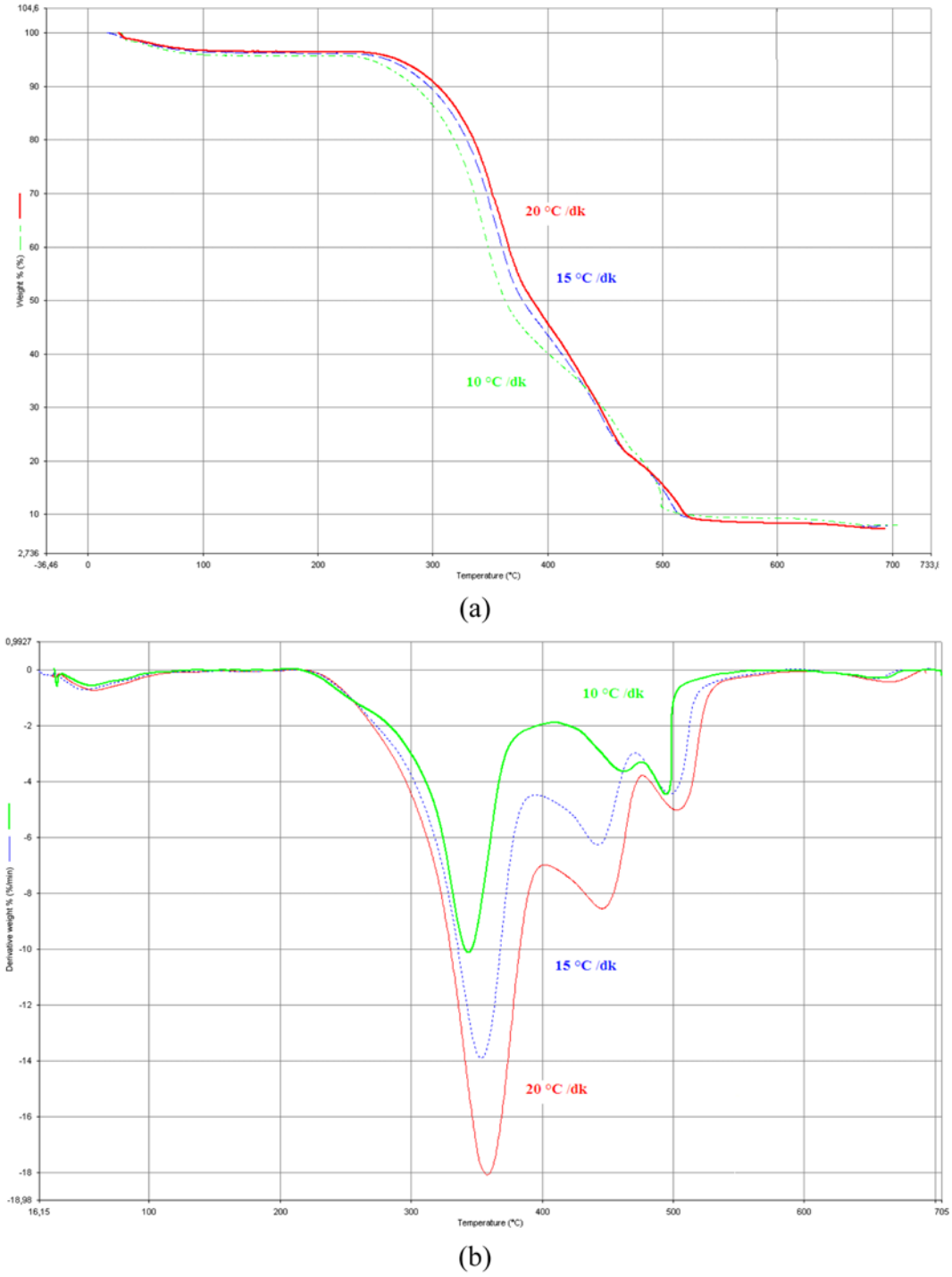

Fig. 7. TG and DTG profile of thermal degradation of the tetra pak panel board at different heating rates, (a) TG, (b) DTG.

given WTPP and TPPBs in Fig. 7 and Fig. 8, respectively. Data obtained through interpretation of TPPBs profiles is given in Table 3.

The TG system was coupled with the FT-IR system and a time-based experiment can thus be performed to analyze the volatiles during the thermal degradation (CH_4, H_2O, CO, CO_2, etc.). FT-IR plots of gas evolution determined at different heating rates are given in Fig. 9. IR absorbance of CH_4, CO_2, COOH, and CH_3OH at maximum reaction rates of the thermal degradation steps are determined and listed in Table 4.

In the present study, the thermal degradation reaction of the TPPB samples can be defined as below:

$$TPPB_{(s)} \rightarrow Volatiles_{(s)} + Char_{(g)} + Aluminum\ Foil_{(s)} \quad (1)$$

Kinetic analysis of thermal degradation reactions of the TPPB samples was done by using mathematical equations of Coats-Redfern, which are non-isothermal kinetic models based on multiple heating rates.

According to the Coats-Redfern method, values of [log(−log(1−α)/

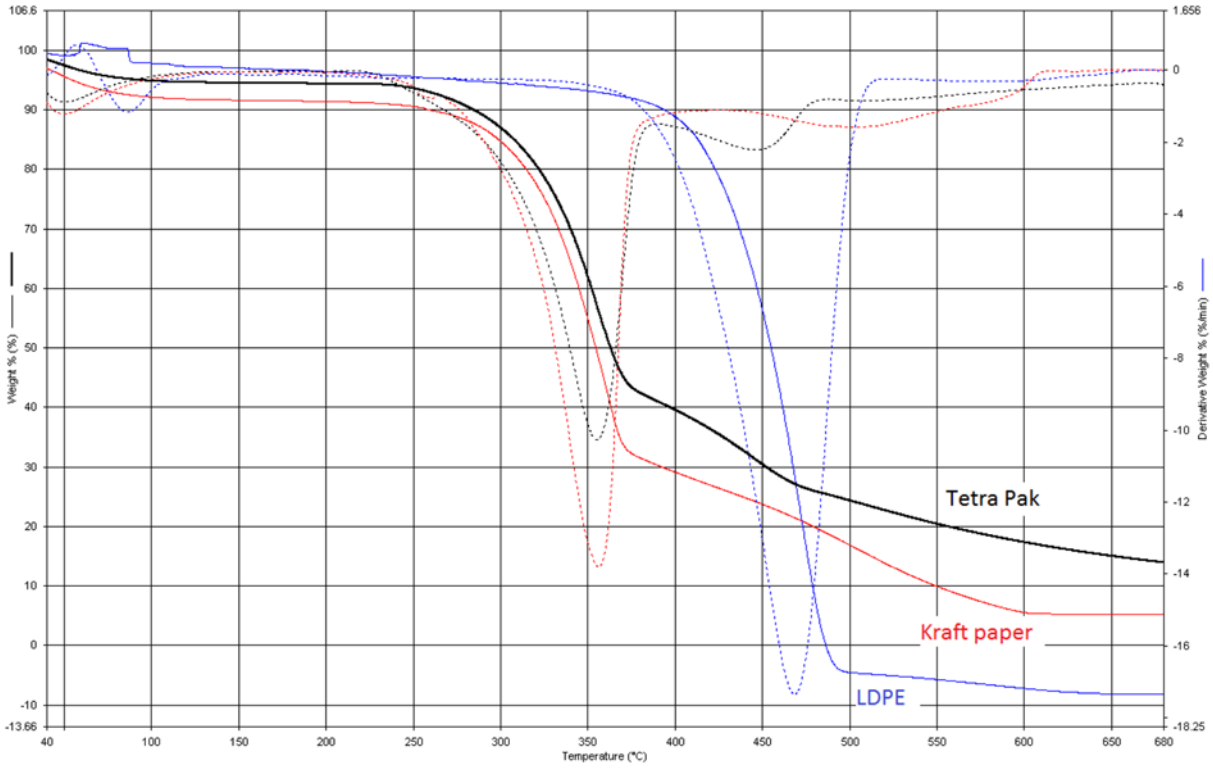

Fig. 8. TG and DTG profile of thermal degradation of the waste tetra pak packages and its components.

Table 3. Characteristic temperatures and mass losses for the thermal degradation reaction of the tetra pak panel board

Reaction steps	Heating rates (°C/min)					
	10		15		20	
	Ti -Tf (°C)	m %	Ti-Tf (°C)	m %	Ti-Tf (°C)	m %
Moisture evaporation	28.56-97.09	3.691	29.08-109.77	2.700	33.30-111.85	2.313
1. Step	204.68-380.52	51.395	207.71-391.88	50.349	219.10-401.26	51.067
2. Step	380.42-476.83	22.780	391.88-471.96	24.544	401.26-473.33	24.917
3. Step	476.83-499.41	10.142	471.96-520.00	11.551	475.94-531.19	11.271
Total mass lost (%)		88.008		90.145		89.568

T^2)] versus 1/T were plotted. The slope of the line was used to calculate activation energy (E_a) and also the pre-exponential factor (k_0) was determined from the intercept of the line (Eq. (3) and Eq. (4)). In this method, 1/T should give a straight line with a maximum correlation coefficient (R^2) for a corrected value of order of the reaction (n). In the Coats-Redfern method, reaction orders were assumed to have the values of 0 to 3 in the decomposition fraction (α) and a range of 0.1 to 0.9 [11].

$$\log\left[\frac{1-(1-\alpha)^{1-n}}{T^2(1-n)}\right]=\log\frac{k_0R}{\beta E_a}\left[1-\frac{2RT}{E_a}\right]-\frac{E_a}{2.303RT} \quad \text{for } n\neq 1 \quad (3)$$

$$\log\left[\frac{-\log(1-\alpha)}{T^2}\right]=\log\frac{k_0R}{\beta E_a}\left[1-\frac{2RT}{E}\right]-\frac{E_a}{2.303RT} \quad \text{for } n=1 \quad (4)$$

R^2 values for all the orders were calculated and plotted against the n values as shown in Fig. 10. R^2–n curves have maximum n values corresponding to the more appropriate kinetic mechanism, from which optimal values of the thermal degradation reaction order were calculated. These n values were put in Eq. (3) to calculate the E_a and k_0 values for each of the heating rates (Table 5).

The literature has indicated that the activation energy depends on several parameters such as the heating rate, particle size distribution, atmosphere and crucible type. The kinetic compensation effect (KCE) was evaluated to validate the kinetic data [12-15]. It has been accepted that under different experimental conditions, between the logarithm of the pre-exponential factor ($\ln k_0$) and the apparent activation energy (E_a), a linear relationship is observed. KCE plots of the thermal degradation steps are given in Fig. 11.

According to the thermal analyses, thermal degradation mechanisms of TPPB and WTPP are illustrated in Fig. 12.

RESULTS AND DISCUSSION

1. Crystal Structure, Infrared Vibrational Frequencies and Microstructure of TTPBs

Crystal structure, infrared vibrational frequencies and microstruc-

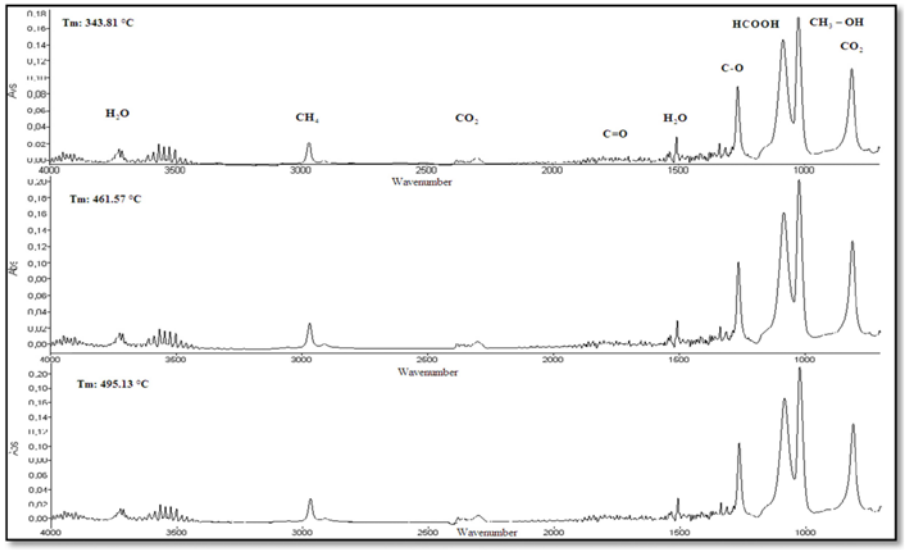

(a) 10 °C/ min

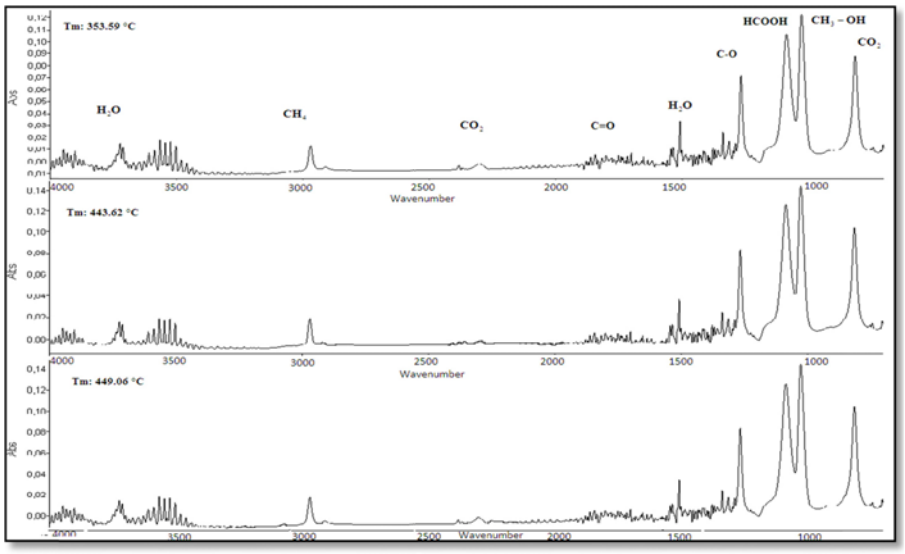

(b) 15 °C/ min

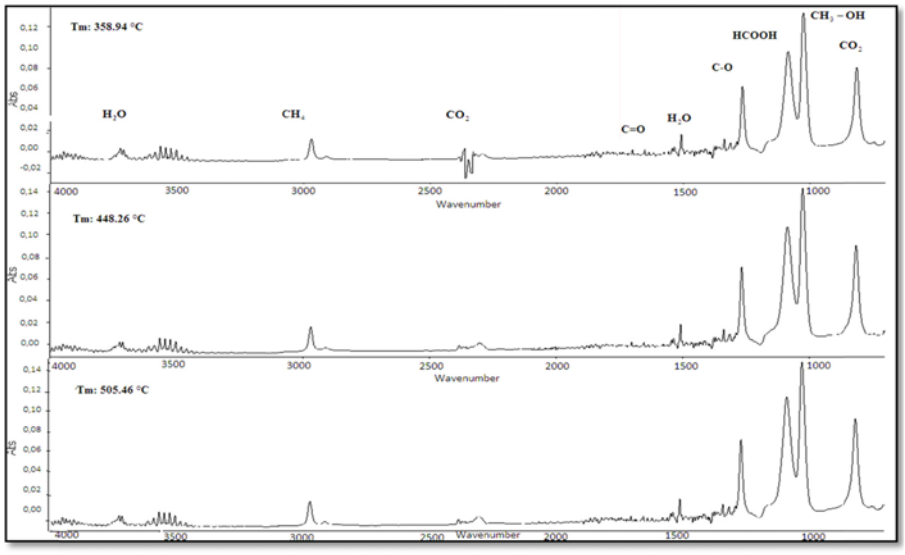

(c) 20 °C/ min

Fig. 9. FT-IR stalks plots at different heating rates.

Table 4. IR absorbance at gas evolution determined via TG-FT/IR in degradation at different heating rate

	Evolved gas	Heating rates (°Cmin^{-1})		
Step		10	15	20
1	H_2O	0,017986	0,017075	0,004864
2	(Absorbance)	0,01817	0,018117	0,005078
3		0,01765	0,018305	0,005437
Step		10	15	20
1	CH_4	0,022695	0,012836	0,012944
2	(Absorbance)	0,01817	0,01658	0,01514
3		0,01765	0,016748	0,016469
Step		10	15	20
1	CO_2	0,003407	0	0
2	(Absorbance)	0,00399	0	0,001356
3		0,004213	0	0,001792
Step		10	15	20
1	HCOOH	0,1461	0,10605	0,094921
2	(Absorbance)	0,1622	0,12481	0,10838
3		0,16578	0,12591	0,11452
Step		10	15	20
1	CH_3OH	0,179	0,12291	0,10347
2	(Absorbance)	0,20289	0,144	0,1409
3		0,2094	0,14435	0,14913
Step		10	15	20
1	CO_2	0,11195	0,087827	0,081667
2	(Absorbance)	0,12776	0,10361	0,090124
3		0,13047	0,1046	0,095551

ture of the TPPBs were investigated by X-Ray diffraction analysis (XRD), Fourier transform infrared spectroscopy (FT-IR), and a scanning electron microscope (SEM), respectively, in the present study.

The XRD pattern of the TPPBs in the diffraction range 10-80° is shown in Fig. 2. As can be seen, two phases were detected as n-paraffin (PDF: 00-040-1995) and aluminum (PDF: 01-088-3657). Peaks appeared at about 2θ of 38.41°, 44.60° and 65.06°, in the aluminum phase. In addition, peaks appeared at about 2θ of 21.46°, 23.83° and 36.07° in the n-paraffin phase. The plastic layer in the TPPBs was transformed into n-paraffin after the temperature and pressure treatment.

Fig. 3 represents the FT-IR spectra and the fundamental peaks of the TPPBs are marked. The FT-IR spectra of the TPPBs were used to determine the vibration frequency in the functional groups. Generally, the peaks observed at about 3,333 cm^{-1} can be attributed to the existence of free and intermolecular bonded hydroxyl groups. The absorption peak of around 2,916 cm^{-1} and 2,849 cm^{-1} indicates the stretching vibration of the C-H band. The peak at around 1,639 cm^{-1} is due to the C-C band stretching vibration, and the peak at 1,465 cm^{-1} corresponds to the C-C stretching vibration. The peak at around 1,158 cm^{-1} is due to the C-O-C band stretching vibration. The strong band at around 1,029 cm^{-1} is due to the C-O group and confirms the presence of Kraft paper in the sample. Also, the peak at around 717 cm^{-1} is attributed to the stretching modes of C-C [16].

SEM is used to visually observe the physical qualities and micro-

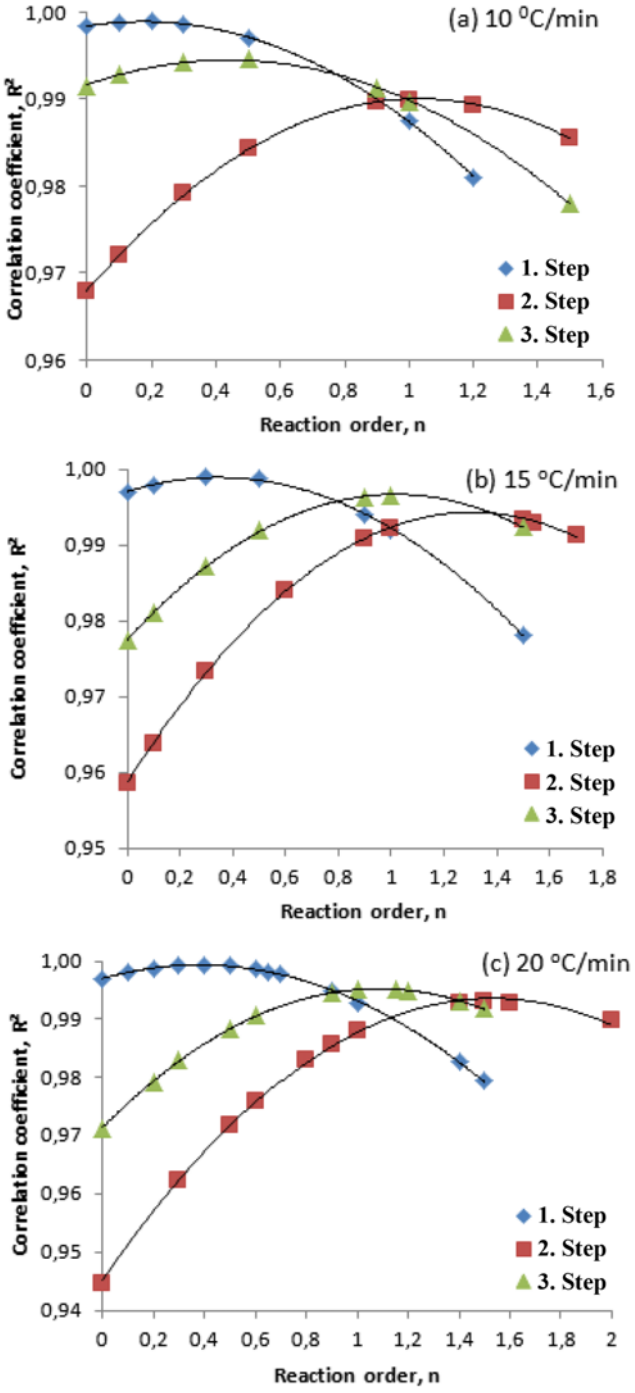

Fig. 10. R^2–n values for Coats-Redfern method at different heating rates.

structure of the TPPBs and its individual components: (a) TPPB, (b) kraft paper, (c) LDPE, (d) aluminum. SEM images at 500× magnification of the samples are shown in Fig. 4.

2. Thermal Degradation Behaviors

The TPPBs were separated into layers of LDPE, Kraft paper and aluminum. Thermal degradation of the TPPBs and their components was carried out under the same conditions to determine the thermal degradation behaviors.

TG, DTA and DTG profiles of Kraft paper and LDPE at 10, 15 and 20 °C/min are given in Fig. 5. Obviously, there were two princi-

Table 5. Kinetic parameters calculated from Coats&Redfern model

Heating rate (°C/min)	Step	Reaction order	R^2	E_a (kJ/mol)	k_0 (min^{-1})
10	II	0.17	0.9989	74.84	3.32×10^{5}
	III	0.35	0.9992	129.14	7.04×10^{8}
	IV	0.40	0.9994	573.06	7.29×10^{38}
15	II	1.00	0.9899	80.62	1.35×10^{6}
	III	1.30	0.9941	201.87	4.94×10^{11}
	IV	1.53	0.9930	399.99	1.06×10^{27}
20	II	0.45	0.9946	85.82	4.82×10^{6}
	III	1.02	0.9967	243.84	4.94×10^{11}
	IV	1.09	0.9951	375.33	1.85×10^{25}

pal reactions observed in the two distinct mass changes over the temperature ranges 200-600 °C for all three heating rates, and a higher heating rate shifted the curve to a higher temperature range as can be seen in the TG curve. It is clear that the degradation of Tetra Pak components was independent of the heating treatment. In addition, DTA curves of Kraft paper indicated that thermal degradation occurred in two endothermic reactions as expected. Kraft paper consists mainly of cellulose along with the hemicelluloses (nearly 5%) and lignin (nearly 5%) and some pulping chemicals such as $CaCO_3$. The first pyrolysis reaction contributed mainly to the degradation of cellulose, hemicelluloses, and lignin and impurities at temperatures between 200-350 °C with a peak of about 350 °C, which belongs to the degradation of cellulose dominantly [17]. The first step is cleavage of glucosidic bond and initial products occur at a lower temperature, and levoglucosan is the most significant primary degradation product of cellulose and furan and furan derivatives such as 1,6-anhydroglucofuranose, enones occur following levoglucosane [18,19]. There is a correlation between increasing temperature and the occurrence of levoglucosane. It is well known that generation of levoglucosane occurs in the crystalline areas of cellulose, and heat treatments lead to increasing of crystallinity of fibrous cellulose [19]. On the other hand, carbonyl groups also were formed in the nitrogen atmosphere and their concentration reached at a constant level after a rapid increase [20]. Besides the cleavage of molecular chains of cellulose, there are also dehydration and oxidation reactions by heat treatment of cellulose [19]. Since pyrolysis in the study was performed in N_2 atmosphere, any possible oxidation reactions were ignored. Even though the sensibility of the hemicelluloses to heat treatment is greater than cellulose, the decomposition and depolymerization of the hemicelluloses in nitrogen atmosphere occur at higher temperatures compared to normal atmospheric conditions. The major decomposition products of the hemicelluloses are methanol, acetic acid, furfural and carbon dioxide, which occurs at elevated temperatures between 200-300 °C [19]. After heating the Kraft paper to 550 °C, the second pyrolysis reaction was observed due to decomposition of intermediates and solid residues with a peak of about 340 °C. This peak can be attributed to the degradation of lignin; dominantly, pyrolytic degradation of lignin occurs at temperatures between 300-450 °C and some of the phenolic compounds are converted into vapor phase [20-22].

The trends of the LDPE TG curves were similar to those of the Kraft paper pyrolysis in the two reaction stages. When the temperature reached about 300 °C, weight loss began and proceeded until 530 °C was reached. Also, higher heating rates shifted the curve to the higher temperature range. From the TG and DTG analysis results, there was no solid residue remaining for 15 and 20 °C/min heating rates while was solid remaining about 20% for 10 °C/min. On the other hand, DTA curves of LDPE indicated that thermal degradation occurred in two endothermic reactions as expected.

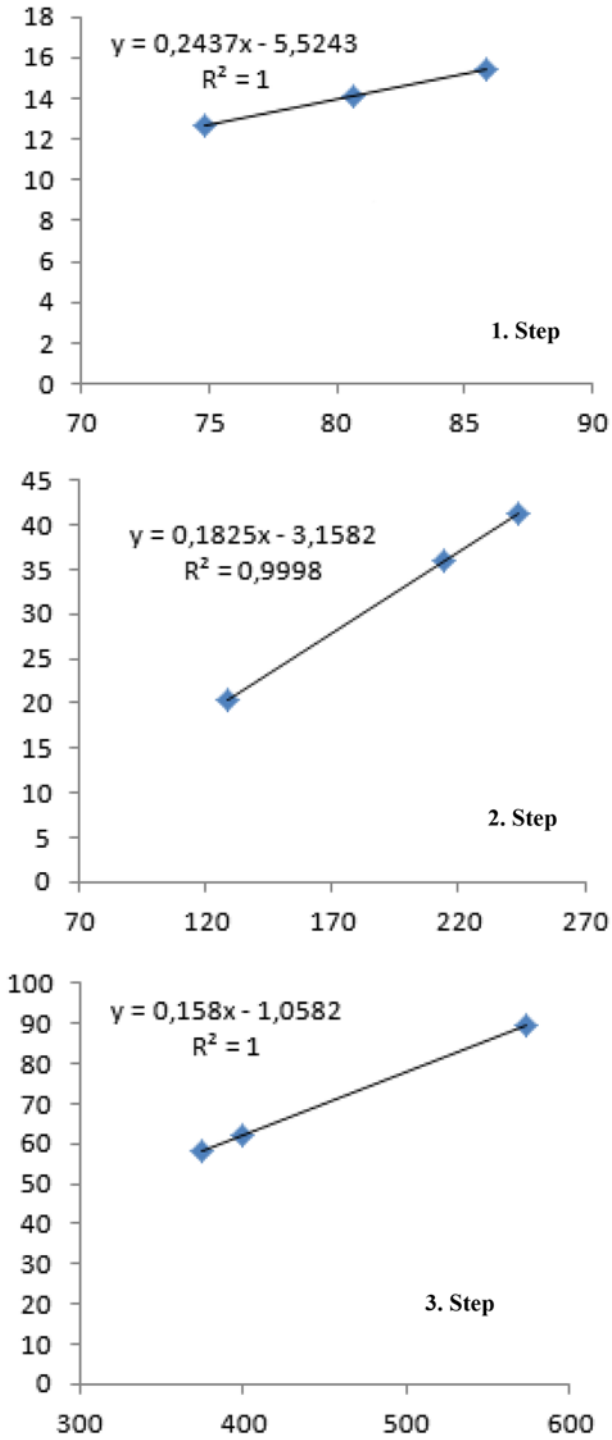

Fig. 11. Kinetic compensation effect for Coats-Redfern method.

It can be seen that the thermal degradation of the TPPBs can be divided into three phases after moisture evaporation. A comparison of

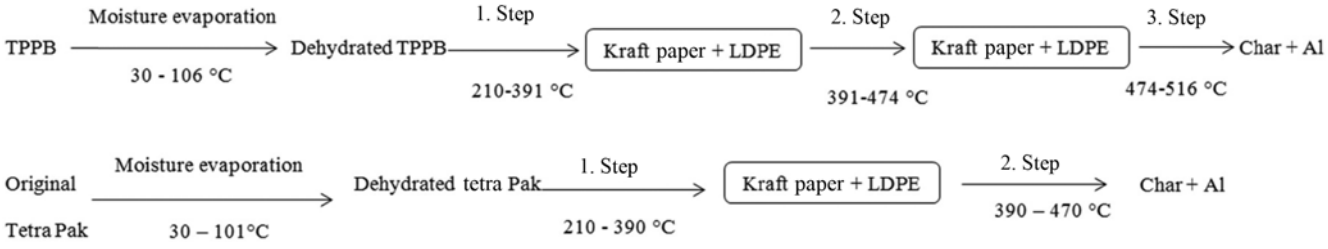

Fig. 12. Thermal degradation mechanism of tetra pak panel board and waste tetra pak packages.

the TG and DTG curves at a 15 °C/min heating rate of the TPPBs, Kraft paper and LDPE is given in Fig. 6. The TPPBs are materials of three different components and their overall thermal degradation behavior can be explained by the association of these components' thermal properties. Thermal degradation reactions of Kraft paper samples took place in two steps and began to occur at lower temperatures (<350 °C) than both LDPE and the TPPBs. It can be seen that the thermal degradation of the LDPE layer, which took place in the main reaction, peaked at 432 °C and the main reaction was followed by a smaller reaction (470 °C). In addition, aluminum foil doesn't degrade during thermal treatment and melts at around 600 °C. It's seems that aluminum had no effect on the trend of TG and DTG profiles of the TPPBs.

Fig. 7 illustrates the TG and DTG profile of the thermal degradation of the TPPBs at different heating rates, and characteristic temperatures and mass loss of thermal degradation reactions are given in Table 3. After the moisture evaporation with 2.7% mass loss (w/w), thermal degradation of the TPPBs occurred in three steps and the DTG curve exhibited three mass loss steps between 299-500 °C. The first thermal degradation took place between 200 and 400 °C with a maximum peak at 435 °C showing a sharp and maximum weight decrease of 50.4% (w/w) corresponding to the degradation of Kraft paper. Therefore, this stage was accepted as the main thermal degradation phase. The second thermal degradation phase occurred between 400 and 461 °C with a maximum peak at 450 °C showing a weight decrease of about 24.5% (w/w) corresponding to the degradation of the remaining Kraft paper and LDPE. The last peak was associated with the decomposition of the remaining Kraft paper and LDPE layers with a mass loss of about 11.6% (w/w). It is clear that the residue consists of char and aluminum foil after the thermal degradation of the TPPBs.

The heating rate has a significant effect on the thermal degradation of the TPPBs. The increase of the heating rate leads to a less uniform heat distribution and a higher temperature gradient. It can be seen that all characteristic temperatures were shifted to higher values when the heating rate was increased. When the heating rates were increased, the thermal degradation temperatures (T_i and T_f) also increased without affecting weight loss. Parallel weight losses were observed at different heating rates due to the chemical contents.

To investigate the effect on fabrication process on degradation behavior of TPPBs, thermal analyses results were compared with WTTP. Fig. 8 shows the TG and DTG profile of thermal degradation of the WTPP. Mass loss corresponding to loss of moisture occurred below 101 °C according to the DTG curve. Thermal degradation of WTPP exhibited two mass loss steps between 210 and 470 °C. The first step took place 210 and 390 °C showing a sharp weight decrease as 52.88% and it was associated with the decomposition of cardboard layer. The second degradation occurred between 390 and 470 °C with a 15.99% weight lost and corresponds to decomposition of polyethylene. This result is in good agreement with the studies pyrolysis of the Tetra Pak [1].

3. Evolved Gas Analysis During Thermal Degradation

Fig. 8 shows the FT-IR spectra taken at a specific temperature which was detected as the maximum thermal degradation rates (Rm, %/min) of the TPPBs for each of the different heating rates. Qualitative analysis was performed based on region and the peak positions. During the thermal degradation of the TPPBs, gases (CH_4, CO, CO_2, H_2O, CH_3OH, HCOOH and some organics) were easily detected in the specific wavenumber. Some characteristic wavenumbers of gas species were: H_2O (4,000-3,400 cm^{-1}, 1,550-1,350 cm^{-1}); CH_4 (3,000-2,800 cm^{-1}, 1,400-1,360 cm^{-1}); CO_2 (2,400-2,250 cm^{-1}, 680-660 cm^{-1}), CO (2,200-2,000 cm^{-1}) C=O bond of esters, aldehydes, and ketones (1,660-1,820 cm^{-1}) , C-O bond of an unsaturated carbon (1,280-1,260 cm^{-1}).

Table 4 shows the IR absorbance of CH_4, CO_2, HCOOH, and CH_3OH as a maximum thermal degradation rate for each of the heating rate. Considering each heating rate of the TPPBs, the profile of FT-IR spectra were very similar indicating that all exhibit a similar thermal degradation behavior. The spectra for each heating rate were taken from the rate of the most intense mass loss, and the time scale can correspond to the thermal degradation temperature. The amount of gas was evaluated based on Beer's law, which assumes that the absorbance of the components is directly proportional to their concentrations. The gaseous products were evolved in a much narrower range of time as the heating rate increases. Maximum thermal degradation appeared to increase with an increase in the heating rate. Based on the results of evolution determined at step II, it can be said that as heating rates increase, the release of HCOOH, CH_4, and CH_3 is mainly decreased. The amount of CO_2 at 15 °C min^{-1} stayed under detection limits. From all of the gaseous evolution results obtained at step II-III, it was demonstrated that conversion of gases to each other is more random and there is not any relationship between the heating rate and the amount of gas released (Table 4).

4. Kinetic Study

Kinetic studies of the TPPBs at three different thermal degradation stages were investigated based on the Coats-Redfern at multiple heating rates (10, 15, and 20 °C/min). In the Coats-Redfern model, E_a and k_o were calculated after the determination of the corrected value of n from the slope and the intercept of the kinetic plots for steps II, III and IV. In the Coats-Redfern method, reaction orders were assumed to have the values in the α range of 0.1 to 0.9 at heating rates of 10, 15, and 20 °C/min. R^2 values for all the orders were calcu-

lated and plotted against the n values as shown in Fig. 9. R^2–n curves have maximum n values corresponding to the more appropriate kinetic mechanism, from which optimal values of thermal degradation reaction order were calculated. These n values were put in Eq. (3) to calculate the E_a and k_0 values for each heating rate (Table 5). It was observed that there was no general trend in the E_a values from the point of the heating rate. According to Table 5, the E_a values varied from 74-85 kJ/mol for phase II, 129-243 kJ/mol for phase III and 375-573 kJ/mol for phase IV. The lowest activation energy was observed in the second phase for all the heating rates, which was the main thermal degradation step, and also the highest activation energy was observed during the last phase for all the heating rates. The reason for the highest activation energy during the last stage was due to the melting of the aluminum foil in the TPPB structure.

An example of the rate equations of the thermal degradation of the TPPB reactions can be written for 10 °C/min. Rate equations can be written for the other heating rates as similar equations in Eq. (5)-(7).

$$\textbf{Step II:} \quad \frac{d\alpha}{dt} = 3.32\times10^{5}e^{-(74838/RT)}(1-\alpha)^{0.17} \tag{5}$$

$$\textbf{Step III:} \quad \frac{d\alpha}{dt} = 7.04\times10^{8}e^{-(129141/RT)}(1-\alpha)^{1.00} \tag{6}$$

$$\textbf{Step IV:} \quad \frac{d\alpha}{dt} = 7.29\times10^{38}e^{-(573059/RT)}(1-\alpha)^{0.45} \tag{7}$$

As a result of the non-isothermal kinetic analysis, the Coats-Redfern method well represents the thermal degradation of the TPPB reactions. To validate the kinetic data reported in the case of the Coats-Redfern, KCE was applied. The KCE plots of E_a based on the $\ln k_0$ values for each of the heating rates are given in Fig. 10. Kinetic data from the thermal degradation reaction of TPPB given the KCE a high correlation coefficient. Thus, pre-exponential factor and activation energy exhibited the same behavior when the heating rate was changed.

From the TG/DTG curves, kinetic and evolved gas analysis in this study, the TBBP degradation under inert atmosphere, there is a three-reaction model for TBBP degradation as shown in Fig. 12. Shred and hot press at 180 °C processes are applied to produce the TBBP from waste Tetra Pak packages. However, chemical modification was not applied during the fabrication. Although thermal degradation of TBBP consisted of four steps as moisture evaporation and following three degradation steps, WTPP was degraded at three steps which include moisture evaporation and two degradation steps. Also, fabrication process had not changed the initial and final temperatures of overall degradation reaction of TBBP compared with waste Tetra Pak packages. Fabrication process only affected the decomposition steps of Kraft paper and LDPE layers in TBBP. On the contrary of the waste Tetra Pak packages, decomposition of Kraft paper and LDPE layers in the TBBP occurred in two consecutive reactions. From the TG/DTG curves of WTPP degradation in an inert atmosphere a two-reaction model is proposed and results are in agreement with study of Wu and Liu, 2001 [2].

CONCLUSION

The recycling of waste Tetra Pak packages composed of paper, low-density polyethylene, and aluminum is of great recycling significance. We investigated the thermal degradation behavior of "Tetra Pak Panel Boards" produced from waste Tetra Pak packages without any significant recycling process, under inert atmosphere.

Thermal degradation behavior of the TTPBs was studied using a thermal analysis system in a nitrogen atmosphere at different heating rates (10, 15 and 20 °C/min). The Coats-Redfern non-isothermal kinetic model was applied to calculate the thermal degradation kinetic parameters. TG results showed that thermal degradation of TTPB consisted of three distinct steps after the moisture evaporation. The first step was accepted as the main thermal degradation phase (200-400 °C) and corresponding to the degradation of Kraft paper. The second thermal degradation step occurted between 400 and 461 °C and corresponds to the degradation of Kraft paper and LDPE. The last step was associated with the decomposition of the remaining Kraft paper and LDPE layer and it's clear that the residue consists of char and aluminum foil after the thermal degradation of the TPPBs.

The effects of fabrication process on the degradation reaction were investigated and three-reaction model was proposed to illustrate the kinetic behavior of the TPPB under inert atmosphere.

Activation energy values varied from 74-85 kJ/mol for step II, 129-243 kJ/mol for step III and 375-573 kJ/mol for step IV. The highest activation energy was observed during the last phase for all the heating rates. The reason for the highest activation energy value during the last stage was dependent on the melting of the aluminum foil in the TPPB structure. CH_4, CO, CO_2, H_2O, CH_3OH, HCOOH and some organics were detected during the thermal degradation of TPPB. It was observed that the maximum thermal degradation rate occurred at the highest heating rate.

ACKNOWLEDGEMENT

Financial support by the Coordination Unit for Scientific Research Projects of Istanbul University, Turkey is gratefully appreciated (Project No: 6408). The authors also acknowledge YEKESAN, Izmir, Turkey for providing the tetrapak panels.

REFERENCES

1. A. Korkmaz, J. Yanik, M. Brebu and C. Vasile, *Pyrolysis of the Tetra Pak, Waste Manage*., **29**, 11 (2009).
2. C. H. Wu and Y. F. Liu, *Energy Fuel*, **15**, 4 (2001).
3. E. Boer, A. Jêdrczak, Z. Kowalski, J. Kulczycka and R. Szpadt, *Waste Manage*., **30**, 3 (2010).
4. C. H. Wu and H. S. Chang, *J. Chem. Technol. Biotechnol*., 76 (2001).
5. A. V. Shekdar, *Waste Manage*., **29**, 4 (2009).
6. www.tetrapak.com.
7. R. N. Szente, M. G. Schroeter, M. G. Garcia and O. W. Bender, *J. Met*., **49**, 11 (1997).
8. C. M. A. Lopes and M. I. Felisberti, *J. Appl. Polym. Sci*., 101 (2006).
9. www.alcoa.com.
10. http://www.ecoallene.com/page.html?id=11.
11. A. W. Coats and J. P. Redfern, *Nature*, 201 (1964).
12. M. E. Brown, M. Maciejewskib, S. Vyazovkinc, R. Nomend, J. Sempered, A. Burnhame, J. Opfermannf, R. Streyg, H. L. Andersong, A. Kemmlerg, R. Keuleersh, J. Janssensh, H. O. Desseynh, C. Lii, T. Tangi, B. Roduitj, J. Malekk and T. Mitsuhashi, *Thermochim. Acta*,

355 (2000).
13. M. B. Dantas, A. A. F. Almeida, M. M. Concei, Jr. V. J. Fernandes, M. G. Santos, F. C. Silva, L. E. B. Soledade and A. G. Souza, *J. Therm. Anal. Calorim*., **87**, 3 (2007).
14. D. S. Dias, M. S. Crespi, C. A. Ribeiro, J. L. S. Fernandes and H. M. G. Cerqueira, *J. Therm. Anal. Calorim*., **91**, 2 (2008).
15. S. Vyazovkina, A. K. Burnhamb, J. M. Criadoc, L. A. Pérez-Maquedac, C. Popescud and N. Sbirrazzuolie, *Thermochim. Acta*, 520 (2011).
16. B. S. Souza, A. P. Moreira and A. M. Teixeira, *J. Therm. Anal. Calorim*., 97 (2009).
17. S. Soares, G. Camino and S. Levchik, *Polym. Degrad. Stabil*., **49**, 2 (1995).
18. M. V. Ramiah, *J. Appl. Polym. Sci*., 14 (1970).
19. D. Fengel and G. Wegener, Wood-Chemistry, Ultrastructure, Reactions. De Gruyter, Berlin-New York, 319 (1984).
20. F. C. Beall and H. W. Eickner, Madison, Wis., US. Forest Products Laboratory TS801.U493 No.130 (1970).
21. M. Brebu and C. Vasile, *Cell. Chem. Technol*., **44**, 9 (2010).
22. N. E. Mansouri, Q. Yuan and F. Huang, *Bio. Res.*, **6**, 3 (2011).